

REPORT DOCUMENTATION PAGE

Form Approved OMB No. 0704-0188

Public reporting burden for this collection of information is estimated to average 1 hour per response, including the time for reviewing instructions, searching existing data sources, gathering and maintaining the data needed, and completing and reviewing the collection of information. Send comments regarding this burden estimate or any other aspect of this collection of information, including suggestions for reducing the burden, to Department of Defense, Washington Headquarters Services, Directorate for Information Operations and Reports (0704-0188), 1215 Jefferson Davis Highway, Suite 1204, Arlington, VA 22202-4302. Respondents should be aware that notwithstanding any other provision of law, no person shall be subject to any penalty for failing to comply with a collection of information if it does not display a currently valid OMB control number.

PLEASE DO NOT RETURN YOUR FORM TO THE ABOVE ADDRESS.

1. REPORT DATE (DD-MM-YYYY) 12-10-2006	2. REPORT TYPE Final Report	3. DATES COVERED (From – To) 15 July 2005 - 24-Jul-07
--	---------------------------------------	---

4. TITLE AND SUBTITLE Unique Inorganic/Organic Nanocomposites For Infrared Applications	5a. CONTRACT NUMBER FA8655-05-1-3022
	5b. GRANT NUMBER
	5c. PROGRAM ELEMENT NUMBER

6. AUTHOR(S) Professor Asim K Ray	5d. PROJECT NUMBER
	5d. TASK NUMBER
	5e. WORK UNIT NUMBER

7. PERFORMING ORGANIZATION NAME(S) AND ADDRESS(ES) Queen Mary College London Mile End Road London E1 4NS United Kingdom	8. PERFORMING ORGANIZATION REPORT NUMBER N/A
--	--

9. SPONSORING/MONITORING AGENCY NAME(S) AND ADDRESS(ES) EOARD PSC 821 BOX 14 FPO AE 09421-0014	10. SPONSOR/MONITOR'S ACRONYM(S)
	11. SPONSOR/MONITOR'S REPORT NUMBER(S) Grant 05-3022

12. DISTRIBUTION/AVAILABILITY STATEMENT
Approved for public release; distribution is unlimited.

13. SUPPLEMENTARY NOTES

14. ABSTRACT

This report results from a contract tasking Queen Mary College London as follows: This project will explore the properties of formulations deemed to be most promising in terms of, for example, uniformity of particle size and distribution. The study of carrier transport through nanocomposite hybrid structures is of fundamental interest. The mechanism is strongly affected by the charge transfer between different phases within the material and energy level quantisation. A specially designed electrode system fabricated on a silicon substrate will be used for this purpose.. Steady state conduction through samples before and after H2S treatment will be investigated at different temperatures ranging from liquid nitrogen to room temperature both under dark and illuminated conditions. Measurement will provide physically meaningful information regarding the generation-recombination mechanism and the role of PbS nanoparticles. For particles with size in the order of 2 nm, as observed in our preliminary work, we would expect to observe Coulomb blockade phenomena in the room temperature I/V characteristics. This would be an important aspect for future investigations into developing nanotechnological devices. Capacitance voltage characteristics will be obtained to determine the location and type of potential barrier. Macroscopic measurements will also be undertaken in order to investigate charge carrier separation mechanisms in the PbS/phthalocyanine composites. The influence of annealing on the I-V characteristics will also be examined. The reverse breakdown voltage will be monitored in order to test the stability of the structure. Low frequency current and voltage noise measurements will be carried out on nanoparticle PbS films, providing quality assessment of nanocrystalline films. The knowledge of in-plane and through plane conductivity will be useful for determining the anisotropy in transport mechanism.

15. SUBJECT TERMS
EOARD, Nanoelectronics, Nanocomposites, Quantum Dots

16. SECURITY CLASSIFICATION OF:			17. LIMITATION OF ABSTRACT UL	18, NUMBER OF PAGES 18	19a. NAME OF RESPONSIBLE PERSON KEVIN J LAROCHELLE, Maj, USAF
a. REPORT UNCLAS	b. ABSTRACT UNCLAS	c. THIS PAGE UNCLAS			19b. TELEPHONE NUMBER (Include area code) +44 (0)20 7514 3154

YEARLY SCIENTIFIC REPORT

UNIQUE INORGANIC/ORGANIC NANOCOMPOSITES FOR INFRA-RED

APPLICATIONS

FA 8655/05-1-3022

Author: Professor Asim K Ray

The Department of Materials, Queen Mary, University of London

Mile End Road, London E1 4NS

Date: 6 September 2006

Introduction

The incorporation of substituents, particularly alkyl groups, at the 1,4,8,11,15,18,21,24 sites of the phthalocyanine nucleus provides soluble derivatives that are ideal for forming spin coated films¹. TEM images show that the compounds form long columnar supramolecular strands during evaporation of a solution² which may explain why their spin coated films are surprisingly well ordered. Indeed, X-ray diffraction data from examples of films formed from metal-free and various metallated 1,4,8,11,15,18,21,24-octaalkylphthalocyanines indicate layer structuring, ie with column axes parallel to the substrate surface, with the repeat distance a little less than the predicted width of the molecule³. The present work focuses spin coated films of the 1,4,8,11,15,18,21,24-octa-hexyl lead phthalocyanine (PbPc)⁴. The chemical structure is given in Figure 1.

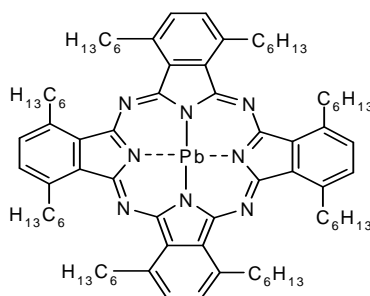


Figure 1: Chemical structure of 1,4,8,11,15,18,21,24-octa-hexyl lead phthalocyanine

The properties of this new class of material, particularly those involving electrical and energy transfer behaviour, are difficult to predict because there appear to be no parallel models available. Nevertheless, the starting point regarding property evaluation will involve investigation of photoconducting and dark conducting behaviour with a view to exploring potentially synergistic effects arising from the formulation.

¹ S.M. Critchley, M.R. Willis, Y. Maruyama, S. Bandow, M.J. Cook and J. McMurdo. *Mol. Cryst. Liq. Cryst.* 1993, **229**, 47-51.

² M.J. Cook. *Chem. Record* 2002, **2**, 225-236

³ S.M. Critchley, M.R. Willis, M.J. Cook and J. McMurdo, Y. Maruyama. *J. Mater. Chem.* 1992, **2**, 157-159,

⁴ A. Auger, W.J. Blau, P.M. Burnham, I. Chambrier, M.J. Cook, B. Isare, K. Nekelson, and S.M. O'Flaherty, *J. Mater. Chem.* 2003, **13**, 1042-1047

Device engineering

Solid-state sandwiched devices were fabricated based on spun-cast films of PbPc, the molecular structure of which is shown in figure 1. PbPc was first dissolved (2 mg/ml) in Tetrahydrofuran (THF) and then Spun-cast on pre cleaned indium tin oxide (ITO) coated glass substrates. To vary the thickness of the films we have deposited films both at a speed of 2000 r.p.m and 3000 r.p.m for 30 sec. The thin films were dried in vacuum ($\sim 10^{-4}$ Torr) at room temperature for 12 h. The thickness of the active layer was around 70 nm for the film deposited at 2000 r.p.m. On top of the dried film, aluminum (Al) from a tungsten filament basket was vacuum-evaporated at a pressure below 10^{-5} Torr. A shadow mask used during Al top electrode evaporation defined the active area of the devices, which were to be 6 mm^2 (the overlap between bottom and top electrodes). The mechanical mask used during Al evaporation also protected the films from excess heat. The devices were kept in a shielded vacuum chamber (10^{-3} Torr) at room temperature for 10 h before a set of current-voltage (I-V) characteristics was taken. The I-V characteristics were recorded with a Yokogawa 7651 dc source and a Keithley 486 picoammeter. In all the cases, bias was applied with respect to the top Al electrode. The voltage was changed in steps of 0.05 V and device current was measured after 1 s, resulting in a scan speed of 50 mV/s. The dc source coupled with fast switching transistors was used to generate voltage pulse of different widths and amplitudes, which were used to “write” or “erase” a state and consequently “read” the states of the devices. Solartron 1260 Impedance Analyzer recorded the impedance characteristics of the devices in a parallel mode. The test voltage of the analyzer was 100 mV rms. Open- and short-circuit compensations were performed with standard normalization procedure in order to minimize the effect of any stray and wire capacitances. The measurements were carried out with SMaRT software. Real and imaginary parts of impedance, Z' and Z'' , respectively, of the devices were measured with and without dc bias. The instruments were controlled with a personal computer via a general-purpose interface bus (GPIB).

Evaluation

We have recorded a set of I-V characteristics of devices based on spun cast films of PbPc sandwiched between ITO and Al electrodes. Voltage was applied in both sweep

directions, and amplitude of maximum voltage (V_{Max}) was also varied. The memory effect of the device is shown in the I - V characteristics of Figure 2. Initially, the as-fabricated device was at its low conductivity state (OFF-state). When the bias voltage was ramped from 0 towards forward bias (V_{Max}) direction, the device current was very low. This low conducting OFF-state continued when the bias was swept back from V_{Max} to negative bias, until at a threshold voltage (-1.53 V), it suddenly switched to high conducting state (ON-state). The figure shows that when the voltage was swept from a negative value, device current was several order higher in magnitude as compared to the current during the other sweep. The conductance switching observed here has an associated memory phenomenon. In other words, the high-conducting state, which is achieved at a negative voltage, is retained when the bias was ramped to positive direction beyond zero. A sufficient positive voltage finally switches the conductivity to its initial low value. When the bias was applied on the device in consecutive loops ($0 \rightarrow V_{Max} \rightarrow -V_{Max} \rightarrow V_{Max}$), the device shows this hysteretic behavior reproducibly except with a little decrease in current value after 4-5 loops. Considering the difference in work-functions of the electrodes used, electron injection in reverse bias becomes favorable resulting to a high-conducting state of the device.

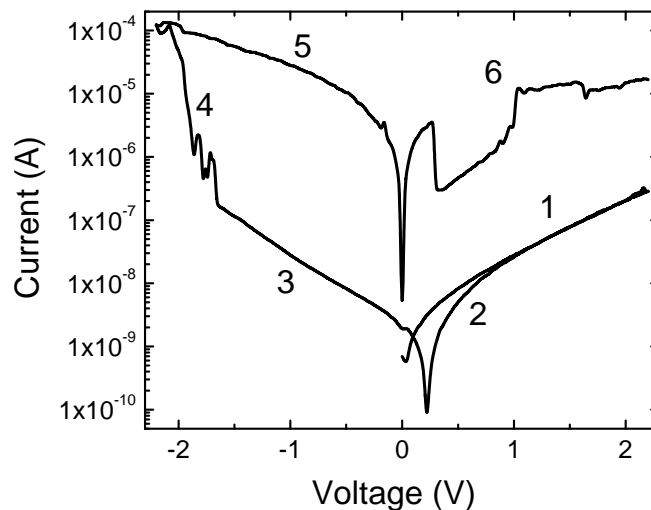


Figure 2. Typical current-voltage (I - V) curves for ITO/PbPc/Al device deposited at 2000 r.p.m during two directions of voltage sweep. Scan rate was 50 mV/s and the numbers show the direction of voltage sweep.

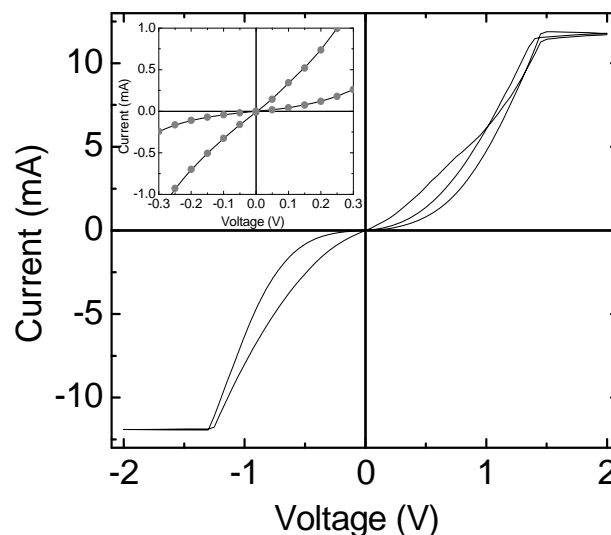


Figure 3. I-V characteristics of a spun cast film of PbPc deposited at 3000 r.p.m and sandwiched between the same electrodes at a scan rate of 50 mV/s. Inset shows the low voltage region of the curve which indicates the ohmic behavior in the ON-state of the device.

We have fabricated single layer memory devices based on spun cast film of PbPc of different thickness by varying the rotating speed of the spinner. Figure 3 shows the I-V characteristics of a comparatively thin film of PbPc deposited on ITO at a speed of 3000 r.p.m for 30 minutes. This figure also demonstrates the memory behavior as depicted by the small hysteresis in the negative bias regime. Being a thinner film as compared to that of the film deposited at 2000 rpm, the current value in the present case is very high, in fact reaching the saturation limit of our instrument. However, the device exhibits an ohmic conduction behavior in the high conducting ON-state in the low bias regime as shown in the inset of Figure 3. The device switched to the high conducting state at a slightly low reverse bias. Due to the lower thickness of the device, the carriers now have to travel less hopping distance to reach from one electrode to other. Since the conductivity is given by the relation $\sigma = \sigma_0 \exp(-R/kT)$, where R is the carrier hopping distance, the device with lesser thickness will show higher conductivity compared to a device with higher thickness.

The I-V characteristic study shows some interesting property at low temperature than at very high temperature. We observed the NDR (negative differential resistance) effect in this material at liquid nitrogen temperature (70K) and this effect is consistent while we go on increasing the temperature. But as the temperature is increasing the effect is

gradually diminishing and is very less at room temperature (300K). The NDR effect may be decreasing but the conductivity is increasing at higher forward bias (at 1.5V) and with increase of the temperature. Apart from showing NDR effect this material shows electrical bistability which is useful for preparing memory devices such as RAM (random access memory) and ROM (read only memory). The bistability of the material is also affected by the change in temperature. We have explained the bistability by fitting with various well established models so that one can predict the mechanism behind the effect. The ac impedance analysis also reveals the same fact. There is increase in the capacitance and the dielectric constant of the material at a particular voltage with the increase of temperature. The Cole-Cole plot gives a perfect semicircle which implies that the circuit is a combination of parallel R-C circuit.

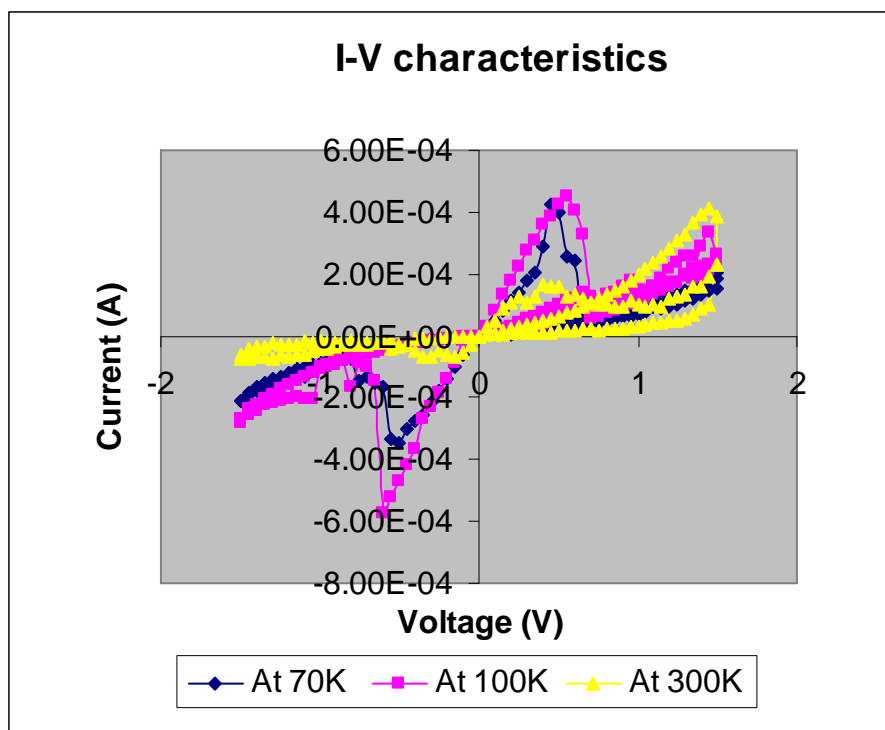


Figure 4. I-V characteristics of a spun cast film of PbPc at different temperatures

Organic memory device

We also have observed an associated memory effects in these switching devices. The active material retained its high-conducting state till a reverse voltage bias erased it. Such a memory phenomenon can lead to data-storage applications in these device structures. In

Fig. 3, we represent random-access memory (RAM) applications of an ITO/PbPc/Al device. The two states have been induced repeatedly by applying a suitable voltage pulse, and probed by measuring device current under a small voltage pulse. In a pristine structure, a -2.5 V for 5 s pulse was applied to “write” the high-conducting state. The state was probed by a -0.5 V pulse (width = 2 s) and measuring the current. The high-conducting state was “read” by measuring the current of the device once in 2 s for 5 times. A $+2.5$ V pulse was then applied to “erase” the high-state and switched to a low-one, which has again been probed or “read” by the same -0.5 V pulse. The whole sequence of “write-read-erase-read” has been repeated for many cycles. In the upper panel of the figure voltage sequence is shown while in the lower panel current response is depicted. The figure clearly shows that the electrical bistability and consequently binary flip-flop of the device between two distinctly different states could be repeatedly observed without any significant device degradation.

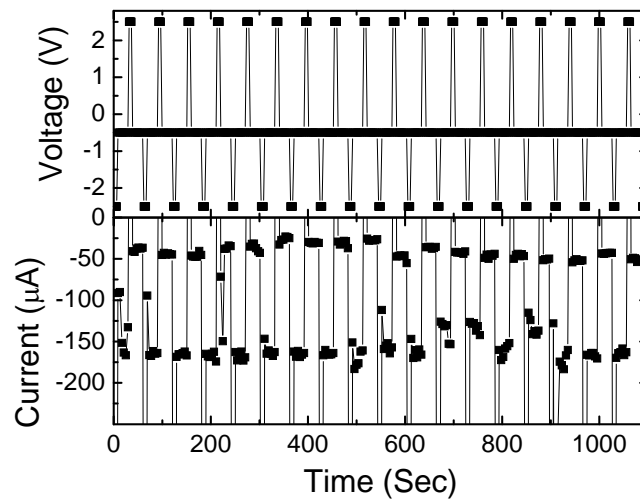


Figure 5. Device current of a spun cast (2000 r.p.m) film of ITO/PbPc/Al based structure under many “write-read-erase-read” voltage sequences. Amplitude of “erase” and “write” voltage pulses have been $+2.5$ V and -2.5 V, respectively. Width of both of them has been 5 s. After “write” and “erase” pulse, the state of the device has been “read” by applying -0.5 V.

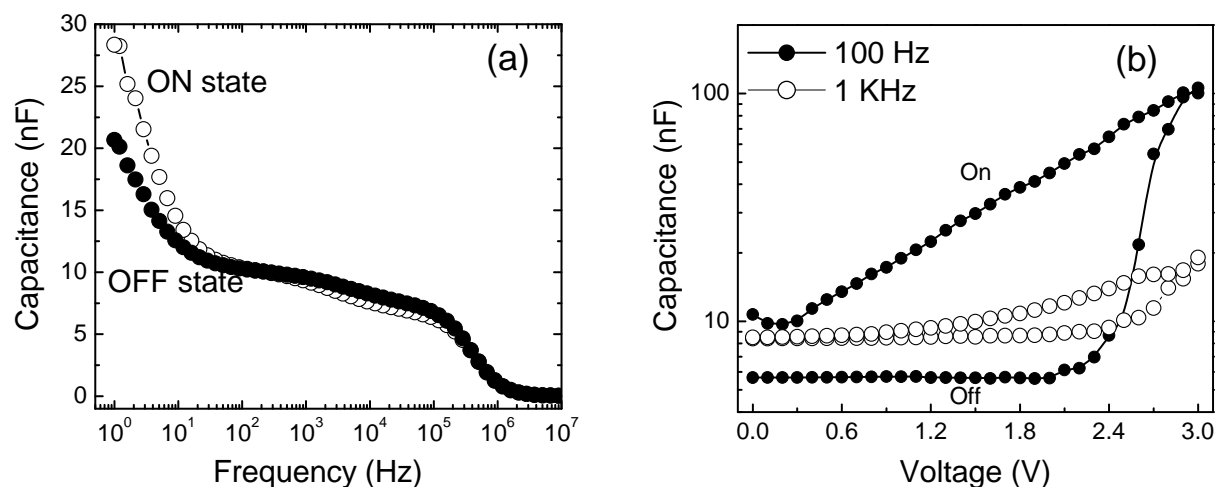


Figure 6(a) Capacitance of the device (measured at 0 V DC bias) as a function of frequency in the two states of the device. ON- and OFF states are represented respectively by open and filled symbols. (b) Capacitance-Voltage (C-V) characteristics of PbPc based film during the conductance transition for two frequency (as depicted in the figure) of the A.C signal. The memory loop decreases with increasing frequency. Only reverse section (amplitude) of the plot is shown for clarity.

The switching mechanism was further studied using impedance spectroscopy. The advantages of dielectric measurements are that it is sensitive to any electrical polarization. The devices can also be modeled to an equivalent circuit. The devices were first switched to an Off- or On-state by suitable voltage pulse. Frequency scans were then made from 12 MHz to 1 Hz at 0 V dc bias keeping magnitude of the test (A.C) signal fixed at 100mV. Real and imaginary parts of complex impedance of the devices in their high- and low-conducting states show semicircular arcs. The devices can hence be modeled to a parallel combination of a resistor and a capacitor network. The diameter of the semicircle, which represents the bulk resistance of the device, shows a large change during the ON- and OFF states of the device. The diameter of the semicircular arc and hence the resistance of the device decreases a lot when the device is in the high conducting (ON) state. The dielectric properties of the device, however, don't show any significant change during the conductance transition (Figure 5a). Figure shows that in the low frequency region, the capacitance of the device becomes slightly greater in the On-state compared to that in the Off-state. Otherwise, the capacitance of the device remains unchanged in both states. We also have measured the capacitance of the devices with

voltage scanning from 0 to $+V_{Max}$ to $-V_{Max}$ and finally to $+V_{Max}$, keeping frequency of the test (A.C) signal as independent parameter. The capacitance of the device also shows a transition at reverse bias and forms a hysteresis loop when voltage is swept back to $+V_{Max}$. The result is depicted in Figure 5(b). Only the reverse bias section is plotted. At lower frequency of the A.C signal, the hysteresis loop is very large and prominent showing a memory behavior. As the frequency increases the loop decreases and finally at very large frequency it disappears. The Figure also depicts that there is a small capacitance difference between the On and Off states of the device when the frequency of the A.C signal is low, e.g, 100 Hz. At higher frequency (1 KHz), the gap disappears.

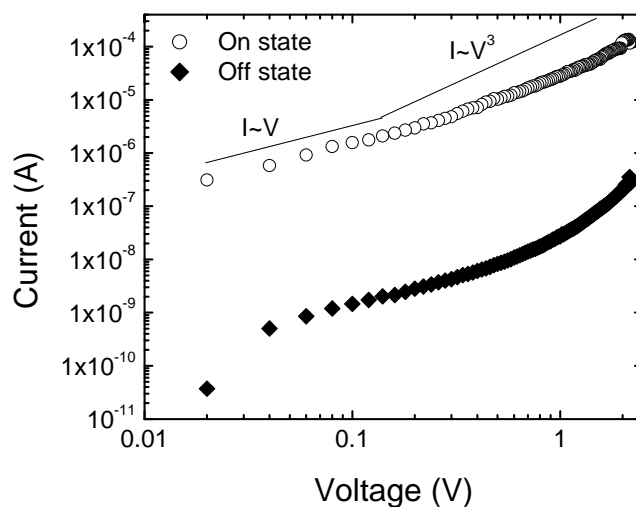


Figure 7. Thermionic emission fitting of an ITO/PbPc/Al device in its high-conducting On-state and low-conducting Off-state. The lines are best fits the experimental points.

We have investigated the transport mechanism by analyzing the I - V relationship. Figure 7 demonstrates the I - V relation at both low and high conducting state for the device. Both states follow $aV+bV^3$ relation meaning that space charge limited current in the presence of deep traps is responsible for the transport

The bistability is attributed to the trapped charge carriers in the bulk of the organic material. At first, these traps are empty, and there are energy barriers at each interface which prevents carriers from being injected into the device. Since holes are the majority carriers in PbPc they will be injected within the bulk of the device at reverse bias. After the carriers being injected at reverse bias, they are trapped within the traps in the bulk, forming space charge as well as large electric field and the voltage drop across the

electrode-organic interface, lowering the interface barrier even though the external bias is removed. As sweeping to the positive, a part of the trapped charges are released, creating some empty traps and then the conductivity is reduced. These empty traps can be charged again as sweeping back to the negative.

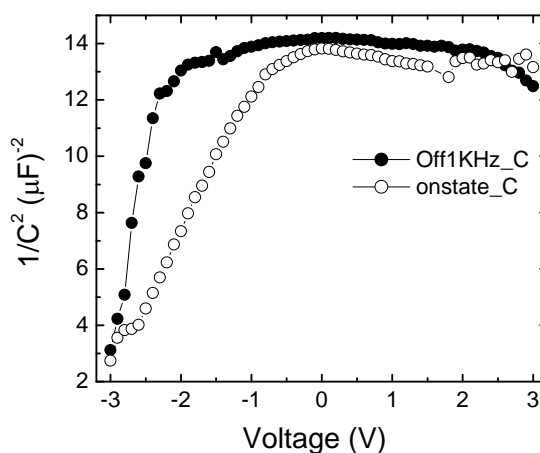


Figure 7. $1/C^2$ Versus Voltage plots for On and Off states of the device

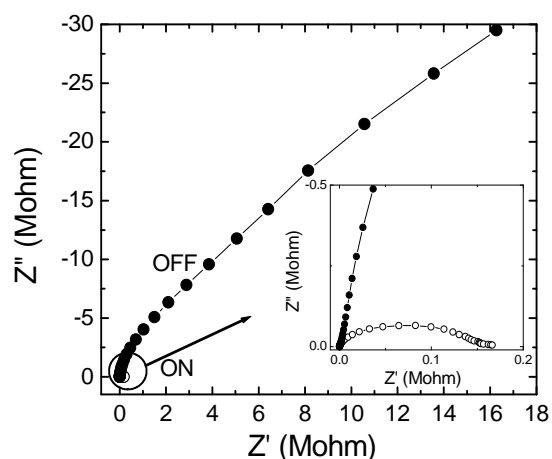


Figure 8. Imaginary versus real part of complex impedance (Cole-Cole plot) of PbPc-based devices deposited at 2000 r.p.m. Plots with 0 V dc bias are shown for high- and low-conducting states (represented by open and filled symbols, respectively). Inset shows the magnified view of both ON and OFF states.

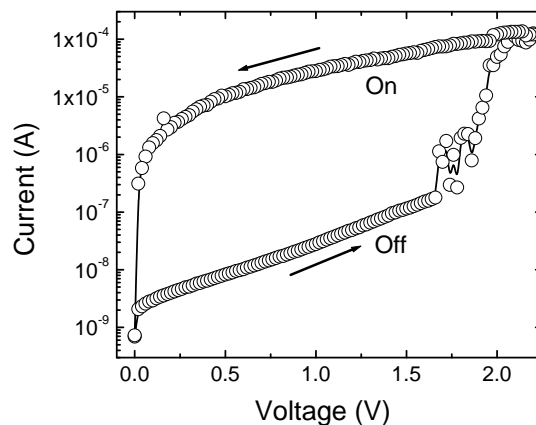


Figure 9. I-V characteristics of the PbPc film for high conducting (On) and low conducting (Off) states of the device. Only reverse bias section (absolute value) is plotted in the figure.

Formation of hybrid nanocomposites

Using the recipe described earlier⁵ the formation of a nanostructured composite material of lead sulphide in a phthalocyanine matrix has been achieved by exposing spin coated PbPc films to H₂S gas for at least 12 h. Further UV-visible spectra were obtained before and after the H₂S treatment of thin films (see Figure 10).

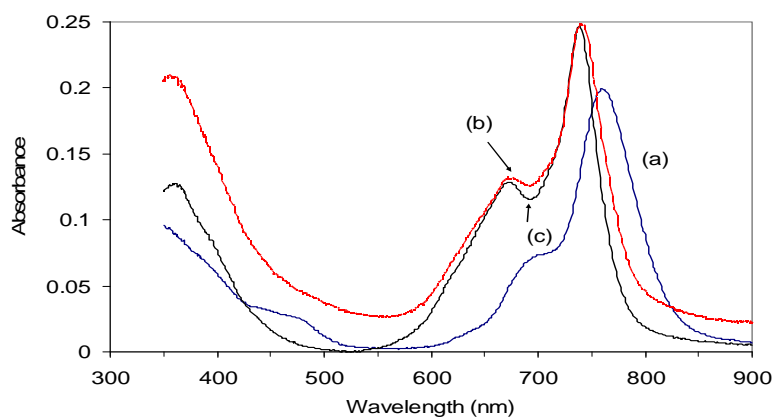


Figure 10: Spectra of (a) a spin coated film of PbPc; (b) after exposure to H₂S over 48 h to metal-free pc (c) an authentic film of pure metal free phthalocyanine

⁵ Nabok AV, Ray AK, Cook MJ, et al. IEEE Transactions on nanotechnology 2004;3(3): 388-3

The phthalocyanine molecules are organized in the stack formation within the spun film PbPc matrix. The introduction of lead sulphide nanoparticles in the PbPc matrix after H₂S treatment distorts only the local environment. The reason why PbS semiconductor nanoparticles have attracted intense research interest over recent years is their potential for applications in nanoscale devices that exploit their unique electrical and optical properties as well as their low dimensionality. As the size is reduced below the bulk exciton diameter, the particles display novel physical and chemical properties as a result of the high surface area to volume ratio, the confinement of charge carriers and size-dependent Coulomb interactions. In view of future applications, nanoclusters based upon metal sulfur compounds will find great potential as photocatalysts or as nonlinear optical materials due to their large nonlinear optical coefficients. Among these, lead sulphide (PbS) is a promising material, having a bandgap of 0.41 eV caused by a direct electron transition and a large Bohr radius of the exciton of about 18 nm. The energy dispersive x-ray analysis output, figure 3, confirms a uniform ratio of Pb to S signals at various sites, a ratio consistent with a previously published report on PbS nanoparticles by Chen⁶ et al. Because of time constraint, we have concentrated on low frequency noise measurements on these hybrid PbS/H₂Pc nanocomposites. Low frequency current noise characteristics normally indicate a random walk (diffusion) phenomenon of carrier between the particles and it is, therefore, possible to predict the size of nanoparticle⁷.

The current noise power spectral density was evaluated for treated and untreated devices in sandwich structure. Since both devices have input resistance greater than 10 k Ω , a transimpedance method, was chosen. The device was placed in series with the transimpedance amplifier and the fluctuations in the dc current were measured by biasing the device at a constant voltage. As the first step, the system background noise was measured. This was necessary in order to investigate the resistance/conductance behaviour of the device when not in bias. When no bias was applied to the device neither flicker nor are generation and recombination (G-R) noise expected. The device was said to be at thermal equilibrium and only exhibited thermal noise (or Johnson noise) of a

⁶ S. W. Chen, L. A. Truax and J. M. Sommers, *Chem. Mater.* 2000, **12**, 3864.

⁷ L.B. Kish, F. Otten, L.K.J. Vandamme, R. Vajtai, C.G. Granqvist, B. Marlow, E. Kruis, H. Fissan, J. Ederth and P. Chaoguang *Physica E*, 2001 **11** (2-3): 131.

conductance $G(f)$. The system background noise was then a system noise floor which was the lowest limit of any measurable measurements. Any noise level which is lower than this value will not be detected by the transimpedance amplifier.

From the plot of ac conductance (G) versus frequency (f) it was found that the ac conductivity of the devices are highly dependence on the modulating signal frequency as shown in figure 11. This implies that the thermal noise current power spectra density (PSD), $S_I(f) = 4kTG(f)$, also increases with the frequency.

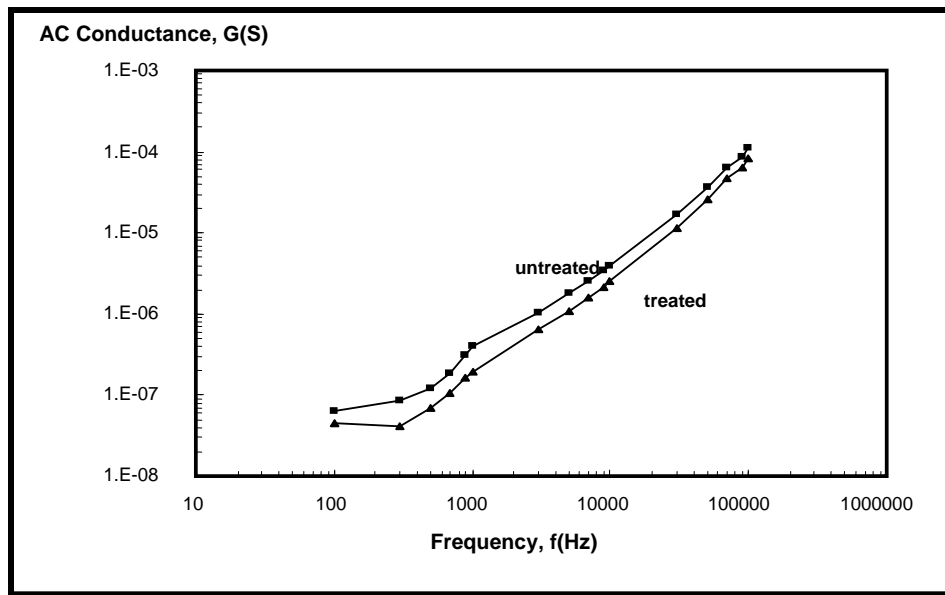
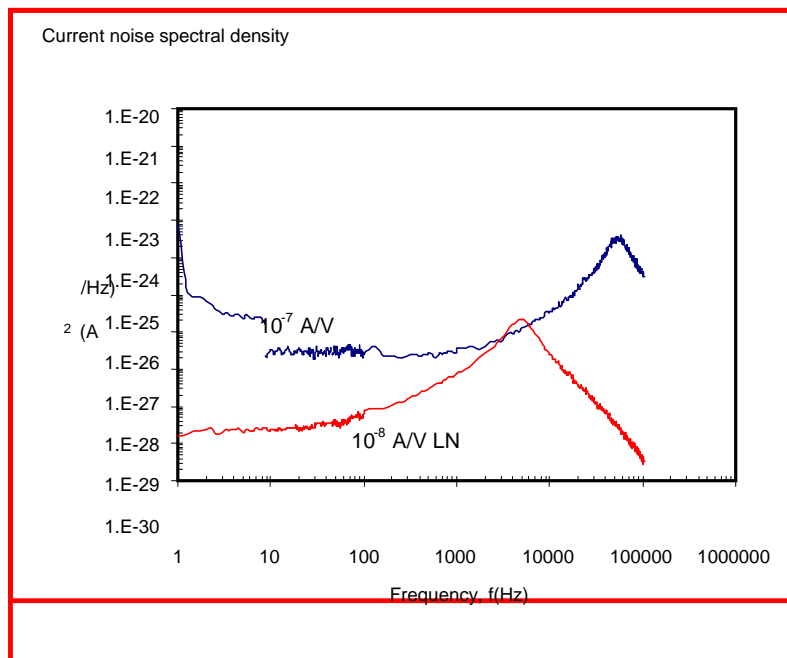


Figure 11. The measured ac conductance (G) of the treated and untreated devices.

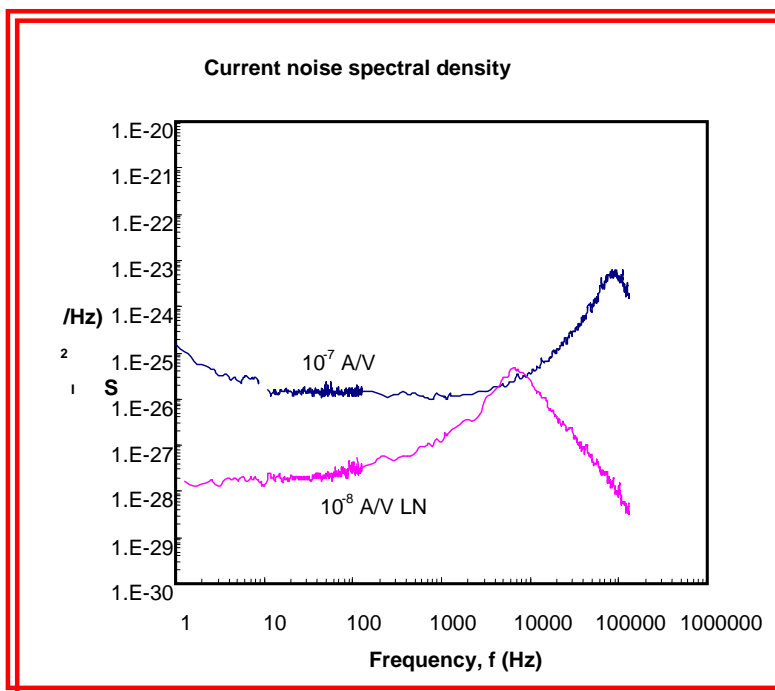
The system background noise for treated and untreated devices were measured by using two different amplifier sensitivity, 10^{-7} A/V and 10^{-8} A/V LN and the results were summarised in Figure 12. From the graph it can be seen that, for the frequency below about 100 Hz for 10^{-8} A/V LN and 1 kHz for 10^{-7} A/V, the system background noise was solely due to amplifier noise. This shows that the background noise was much lower than the amplifier background noise thus cannot be resolved by the amplifier. Due to bandwidth limitation of the amplifier at its highest sensitivity (10^{-8} A/V LN). The

amplifier gain at 10^{-7} A/V was used for upper frequencies (above ~ 4 kHz) to determine the system background noise. Both structures (treated and untreated) had background noise power spectral densities. These parameters were highly dependent on the frequency. Because of this, the lowest level of measurable noise was limited by the system background noise. This was regarded as being the thermal noise of the structures.

Figure 13 shows the current noise power spectral density (PSD) of untreated and treated devices as a function of frequency for different forward bias current. Noise spectra of $1/f$ type was observed experimentally over more than 4 orders of magnitude of frequency range for both devices for the whole range of leakage current. Noise PSDs were found to decrease with frequency but increase with bias current. For the same value of dc current, treated device was found to have current noise PSD approximately two orders of magnitude higher than untreated device. This was expected since by

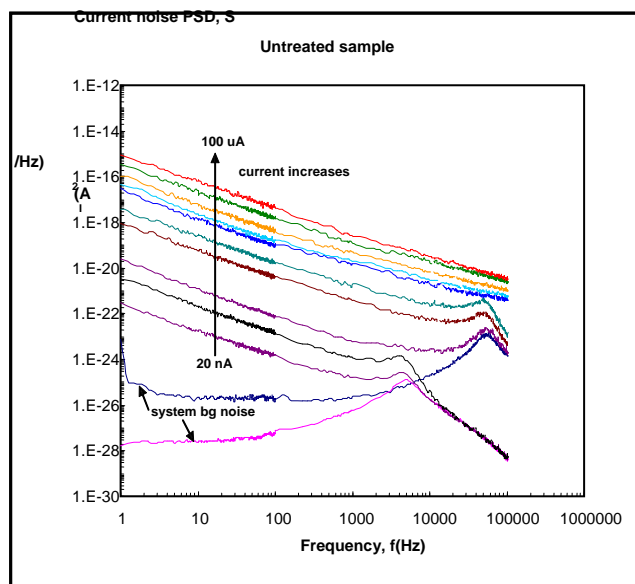


(a)



(b)

Figure 12 The measured system background (Johnson) noise for PbPc before and after H₂S treatment. incorporating PbS nanoparticles into Pc matrix the surface structure of the films had changed as seen on AFM. Nevertheless such complicated structures still have noise behaviour comparable to ordinary devices.



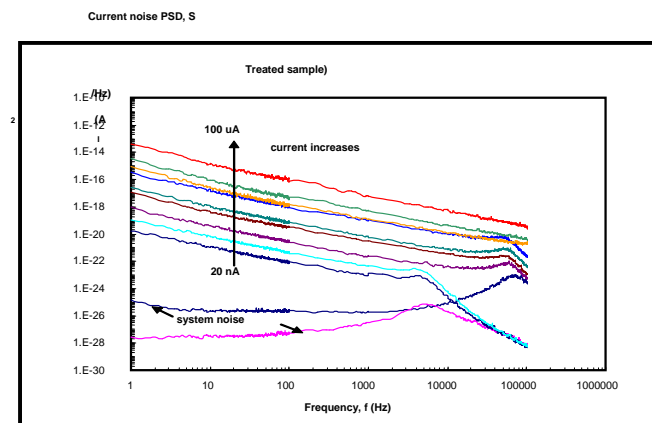


Figure13. Current noise spectral density for PbPc samples before and after H_2S treatment. System background noise are shown as reference.

Concluding Remarks

Electrical measurements on untreated lead phthalocyanine films is now complete and some novel device properties have been demonstrated. New nanocomposite is also formed mixing single walled carbon nanotubes with spun films of lead phthalocyanine molecules and electrical characterization of these nanocomposite is performed.

Large scale arms smuggling for malevolent acts has now become a major security threat. Governments all over the world are anxious to strictly regulate the manufacture, import and sale of arms and weapons. Permanent UV pens and ink markers are commercially available but do not deter highly organised traders from unscrupulous dealings. Invisible inscription is regarded as being a powerful preventive tool for gun crimes. While humans may see in the visible spectral region, our ability to visualize threats to our safety depends upon mastery of the infrared spectral region. The present work demonstrates the feasibility of the general strategy for the formulation of a unique hybrid inorganic-organic nanostructured material by embedding infrared inorganic PbS quantum dots into functional macrocyclic matrices for security tags. Information obtained from electrical measurements on charge transfer, separation and recombination processes at the PbS/Pc interface are crucial for the read and write capabilities of invisible inscription on the tags.

Visitors involved in the Project

1. Mr. Biswanath Mukherjee from Indian association for Cultivation of Science

2. Mr Satyajit Sahu from Indian association for Cultivation of Science
3. Ms. Moumita Santra from Jadavpur University, Kolkata

Publications in 2005/2006

1. A. Bandyopadhyay, A.K. Ray, A. K. Sharma and S. I. Khondaker “**Charge transport through neural network of DNA nanocomposites**”, *Nanotechnology* 17, 227-231, 2006
2. B. Pradhan, A. K. Sharma and A.K. Ray, “**Optical studies on chemical bath deposited nanocrystalline CdS thin films**” *Journal of Nanoscience and Nanotechnology* 5 (7); 1118–1122, 2005.
3. B. Pradhan, A. K. Sharma and A.K. Ray “**Fabrication of nanoscale films of organic dyes for environmental sensing**” *Sensors and Actuators (submitted)*.
4. B. Mukherjee A. K. Sharma and A.K. Ray “**Charge transfer through Single molecule : theoretical background and different techniques**” *IEE: Circuits, Devices and Systems (submitted)*

Appendix

Reprint of three articles